Summary of Supplementary Materials:

1) Materials and Methods.
2) Table S1 – list of signature genes (Word format).
3) Table S2 – reagent table (Word format).
4) Supplementary figures and descriptions (a total of 8).
5) References.

Materials and Methods:

Islet cell preparation, sc-RNAseq, and DNA methylome assays

*MNYA i*slet isolation and dissociation followed that in Methods of the manuscript to purify the β cells for pseudo-islets (PSI) production and assays. Sc-RNAseq and DNA methylome assays were also described in the method section in the manuscript.

ADP/ATP assays

Islets were isolated from 2-3-month-old mice (males and females in equal proportion) using FACS. They were then incubated with RPMI1066 with G2.8 or G20 (with 10% FBS) at 37 °C for 15 minutes and lysed for ADP/ATP ratio assays. The assay used an ADP-Glo™ Max Assay kit from Promega.

***In vitro* pancreas bud culture assay**

As shown in [1], E14.5 pancreatic buds were dissected and cut into 3-4 pieces. They were then cultured in complete RPMI1066 media on filters in an air-liquid interface format with DMSO or 2 μM Aza-Cytidine. About 48 hours later, the tissues were prepared as frozen sections and used for immunofluorescence assays using antibodies in the reagent table. **I**mmunostaining followed standard protocols, as in [1].

Cell line usage

AlphaTC6 (a gift from Wenbiao Chen of Vanderbilt University, School of Medicine) was maintained in DMEM (low glucose) with 1X glutamine, 1X nonessential amino acids, 1X antibiotics, and 10% FBS. They were used to examine the Arx expression upon DNA methylation. Briefly, freshly seeded cells were transfected with a plasmid expressing a gRNA (sequence shown Fig. S3g) and another plasmid expressing dCas3-Dnmt3a (Addgene, #71666, co-expressing eGFP) using lipofectamine. 5 days after transfection, $eGFP^+$ cells were sorted and analyzed for *Arx* expression using QRT-PCR using oligos (5'-acgacttcctccaggactatac -3'. 5'-ggctgtcaccaactacttcaa -3'). Controls for QRT-PCR were GAPDH, with oligos described in manuscript.

Movie-S1: An example of real-time imaging of GCaMP6 of a few female MNA islets. The recording interval is 5 seconds. Basal glucose is 1 mM. Stimulatory glucose is 11 mM, added 5 minutes after the recording started. The images used to identify tdT^- and tdT^+ cells are presented in Fig. S3D.

Table S1. The 20 DEGs between mouse β-cell subtypes that were used for classifying human β cells. The references that support the stated roles of genes are provided here. Related to Fig. 8.

CHGA	Vesicle production [2]
EEF1A1	Stress-related [3]
EIF1	Stress-related [4]
GNAS	Secretion [5]
HINT1	Apoptosis regulator [6]
HSP90AB1	Stress-related [7]
INS	Vesicle production
MT-CO1	Cellular senescence [8]
OAZ1	Cell proliferation [9]
PCSK1N	Hormone processing [10]
PCSK2	Hormone processing [11]
PEBP1	Cell proliferation [12]
RAB11A	Vesicle production [13]
RBP4	Stress-related [14]
RPL17	Protein synthesis [15]
RPL31	Protein synthesis [16]
SOD1	Stress-related [17]
Syt7	Secretion [18]
TPD52	Vesicle trafficking [19]
TPT1	Cell death [20]

Table S2. Key resource table.

REAGENT or RESOURCE	SOURCE	Cat#/Lot #
Antibodies (with fold of dilution indicted)		
488-donkey anti Guinea Pig (1:1000)	Jackson Immunoresearch	706-545-148, 152898 RRID:AB_2340472
488-donkey anti goat igG (1:1000)	Jackson Immunoresearch	705-545-147, 122187 RRID:AB_2336933
Alexa Fluor® 647 AffiniPure Donkey Anti-Guinea Pig IgG (H+L) (1:1000)	Jackson Immunoresearch	706-605-148, 132968 RRID:AB_2340476
Alexa Fluor® 488 AffiniPure Donkey Anti-Rabbit IgG (H+L) (1:1000)	Jackson Immunoresearch	711-545-152, 134352 RRID:AB_2313584
Alexa Fluor® 647 AffiniPure Donkey Anti-Rabbit (1:1000)	Jackson Immunoresearch	711-605-152, 134312 RRID:AB_2492288
Alexa Fluor® 647 AffiniPure Donkey Anti-Mouse IgG (H+L) (1:1000)	Jackson Immunoresearch	715-605-150, 131725 RRID:AB_2340862
Alexa Fluor® 594 AffiniPure Donkey Anti-Mouse (1:1000)	Jackson Immunoresearch	715-585-150, 134514 RRID:AB_2340854
Alexa Fluor® 594 AffiniPure Donkey Anti-Goat IgG (H+L) (1:1000)	Jackson Immunoresearch	705-585-003, 130265 RRID:AB_2340432
Rabbit anti-Syt7	SYSY	#105173, 32101388 RRID: AB_887838
Goat anti-somatostatin (1:500)	ABcam	AB30788 RRID:AB_778010
Guinea pig anti insulin (1:1000)	Dako	A0564, 10115930 RRID: N/A
Rabbit anti-Myt1 (1:1000)	This lab	N/A
Mouse anti-glucagon (1:5000)	Millipore	MabN238, 2769077 RRID:NA
Goat anti-Neurog3 (1:1000)	This lab	NA
Guinea pig anti-Myt2 (Myt1L) (1:1000)	This lab	NA
Rabbit anti-somatostatin (1:2000)	Dako	A0566, 0506 RRID: AB_955424
Rabbit anti-Ki67(1:500)	Abcam	Ab 15580, GR3198179-1 RRID: AB_443209
Rat anti-Myt3 (1:500)	This lab	NA
Rabbit anti-MafB	Gift from R. Stein (Vanderbilt)	NA
Rabbit anti-DNMT3a	GeneTex	GTX33161, 822401956
Rabbit anti-TPT1	ABcam	AB375062, GR1251118-1
Rabbit anti-CD9	Gene Tex	GTx76185, 822401159
Cy5-conjugated Rabbit anti-CD24	In Vitrogen	45-0242-82, 2527401
Cy5-conjugated Rabbit anti-CD79	In Vitrogen	45-0792-44, 2702049

Bacterial and Virus Strains		
Bl-21	Vanderbilt MPB Core	NA
DH5-alpha	Vanderbilt MPB Core	NA
Xl-1	Vanderbilt MPB Core	NA
Biological Samples		
Bovine serum albumin	Sigma	A9418
Donkey Serum	Jackson ImmunoResearch	017-000-121 **RRID:AB_2337258**
Fetal Bovine Serum	Atlanta Biologicals	S10250
Chemicals, Peptides, and other key reagents		
Collagenase from Clostridium histolyticum	Sigma	C5138
DMSO	Sigma	D2650
DAPI	Sigma	**D9542**
Trypan Blue	Fisher Scientific	15250
Adenosine, periodate oxidized	Sigma	7154
5-Azacytidine	Sigma	A2385
paraformaldehyde	Sigma	P6148
Millicell	Millipore	PIHA01250
Trypsin	Sigma	C5138-5G
SuperScript III Reverse Transcriptase	Thermo	18080085
RNaseOUT Recombinant Ribonuclease Inhibitor	Thermo	10777019
Barcoded hydrogel microspheres (BHM)	1cell	
Droplet Stabilization Oil	Droplet Genomics	DG-DSO-20
Cell Barcoding Chip V2	Droplet Genomics	DG-CBC2-80
1H,1H,2H,2H-PERFLUORO-1-OCTANOL, 97% ; used at 20% in HFE	Sigma	370533-5g
Exonuclease I	NEB	M0293L
FastDigest HinFI restriction endonuclease	Thermo	FD0804
Agencourt AMPure XP magnetic beads	Beckman Coulter	A63881
Agencourt AMPure XP magnetic beads	Beckman Coulter	A63881
NEBNext® mRNA Second Strand Synthesis Module	NEB	E6111L

HiScribe T7 High Yield RNA Synthesis Kit	NEB	E2040S
RNA Fragmentation Reagents	Thermo	AM8740
PrimeScript Reverse Transcriptase	Takara	2680B
Deoxynucleotide (dNTP) Solution Mix (10 mM each)	NEB	N0447L
RNaseOUT Recombinant Ribonuclease Inhibitor	Thermo	10777019
Kapa 2x HiFi Hot Start PCR mix	VWR	KK2601
Eva Green Dye	VWR	31000-T
Corning Costar Spin-X	Thermo	CLS8162
Qiagen genomic DNA isolation	Qiagen	69504
EZ DNA Methylation Lightning kit	Zymo	D5030
Tn5 enzyme for methylome DNA tagmentation	Home made	
10X Ampligase Buffer for methylome library construction	Epicentre	A1905b
dNTP for methylome library construction	Thermo	R72501
T4 DNA Polymerase	NEB	M0203S
Ampligase	Lucigen	A3210K
Critical Commercial Assays		
High capacity cDNA synthesis	Applied BIosystems	4368814
SYBER Green qpcr mix	Biorad	1705060
DNA oligos (5' to 3')		
Syt7 guide RNA 1 for CRISPRi in mice	agagagtgtgtgcgcgcccg	N/A
Syt7 guide RNA2 for CRISPRi in mice	agcggcggcagagaagcgcg	N/A
Syt7 guide RNA2 for Syt7 repression in MIN6 cells	gaacatgtggggctccagcg	N/A
RT-PCR-oligos GAPDH-forward	aactttggcattgtggaagg	N/A
RT-PCR-oligos GAPDH-reverse	ggatgcagggatgatgttct	N/A
RT-PCR-oligos Syt7-forward	ctttcgccttcgacataccc	N/A
RT-PCR-oligos Syt7-reverse	ggctgagcttgtctttgtcc	N/A
RT-PCR-oligos Cacna1a-forward	gccttacttccactcttccttc	N/A
RT-PCR-oligos Cacna1a -reverse	aggatgtaccaggtttgatgac	N/A
RT-PCR-oligos Cacna1c -forward	ggcaaccatgtcacctactatc	N/A
RT-PCR-oligos Cacna1c -reverse	cttggttgttccctgtcttgt	N/A
RT-PCR-oligos Cacna2d1 - forward	gtggtttactggactgtggaa	N/A
RT-PCR-oligos Cacna2d1-reverse	ccctttgctctccaccattat	N/A

siRNA pools for gene knockdown		
Non-targeting controls	D-001810-10-05	N/A
Cacna1a	L-043179-00-0005	N/A
Cacna1c	L-040723-00-0005	N/A
Cacna2d1	L-044128-00-0005	N/A
Deposited RNAseq Data		
GSE254702 – Bulk RNAseq in progenitors treated with maternal diet		
GSM8049147	Control_Islet_Progenitor_ HFD-1	
GSM8049148	Control_Islet_Progenitor_ HFD-2	
GSM8049151	Control_Islet_Progenitor_ HFD-3	
GSM8049164	Control_Islet_Progenitor_ND-1	
GSM8049165	Control_Islet_Progenitor_ND-2	
GSM8049166	Control_Islet_Progenitor_ND-3	
GSE254955 – DMA methylomes		
GSM8061312	WGBS of P2 M-N+ (eGFP-) sorted β-cells from female mice - Rep 1	
GSM8061313	WGBS of P2 M+N+ (eGFP+) sorted β-cells from female mice - Rep 1	
GSM8061314	WGBS of P2 M-N+ (eGFP-) sorted β-cells from male mice - Rep 2	
GSM8061315	WGBS of P2 M+N+ (eGFP+) sorted β-cells from male mice - Rep 2	
GSM8061316	WGBS of P60 M-N+ (eGFP-) sorted β-cells from female mice - Rep 1	
GSM8061317	WGBS of P60 M-N+ (eGFP-) sorted β-cells from male mice - Rep 2	
GSM8061318	WGBS of P60 M-N+ (eGFP-) sorted β-cells from female mice - Rep 3	
GSM8061319	WGBS of P60 M-N+ (eGFP-) sorted β-cells from male mice - Rep 4	
GSM8061320	WGBS of P60 M+N+ (eGFP+) sorted β-cells from female mice - Rep 1	
GSM8061321	WGBS of P60 M+N+ (eGFP+) sorted β-cells from male mice - Rep 2	
GSM8061322	WGBS of P60 M+N+ (eGFP+) sorted β-cells from female mice - Rep 3	
GSM8061323	WGBS of P60 M+N+ (eGFP+) sorted β-cells from male mice - Rep	
GSE255135 -ScRNA-seq of single β cells		
GSM8064626	P2_islet_cells	
GSM8064627	P2_islet_cells_repeat_1	

GSM8064628	P2_islet_cells_repeat_2
GSM8064629	P2_islet_cells_repeat_3
GSM8064630	2_month_male_islet_cells
GSM8064631	2_month_female_islet_cells
GSM8064632	2_month_male_islet_cells_repeat_1
GSM8064633	2_month_male_islet_cells_repeat_2
GSM8064634	2_month_female_islet_cells_repeat_1
GSM8064635	2_month_female_islet_cells_repeat_2

Supplemental Figures:

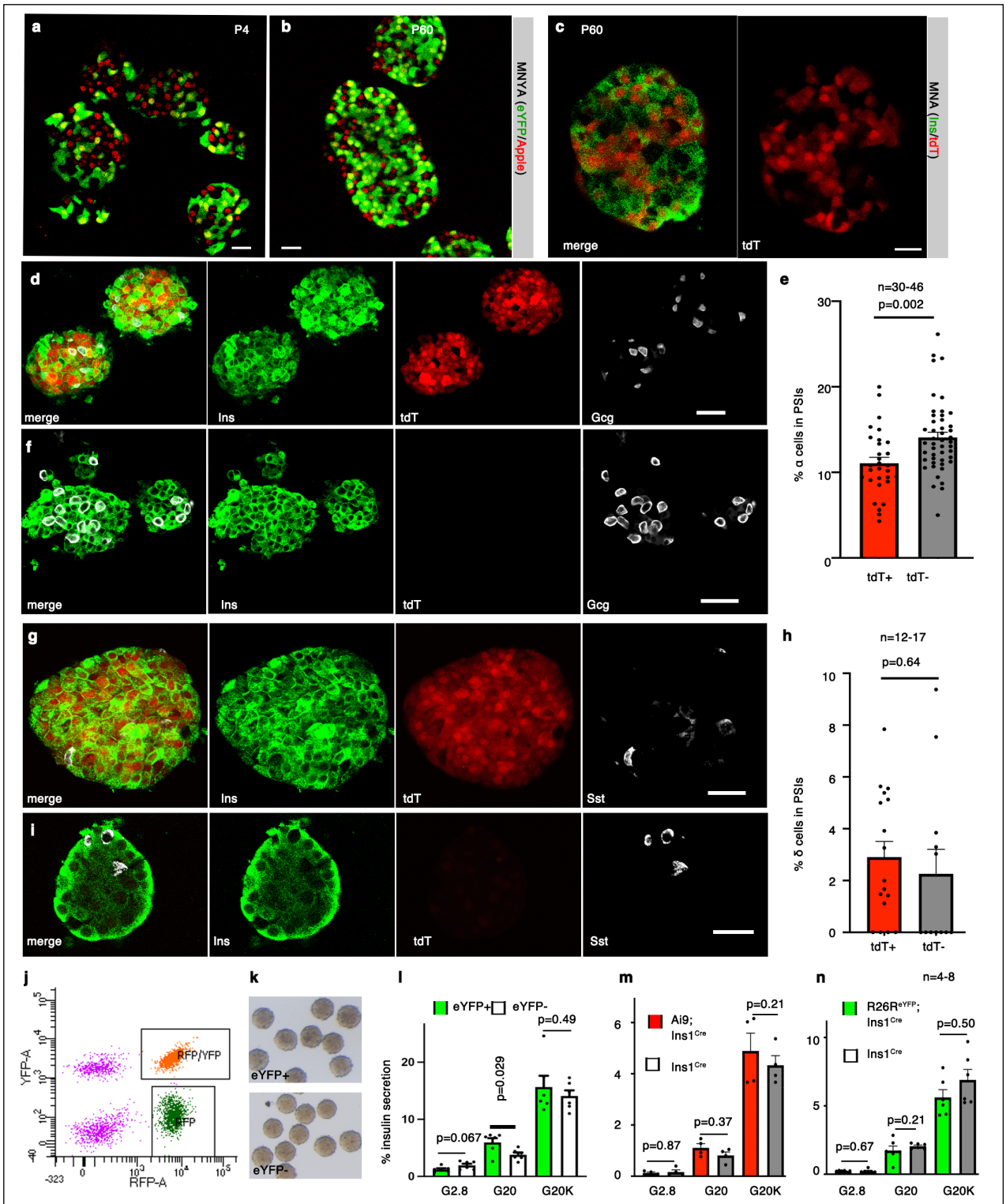

Fig. S1: β-cell subtype secretion and mitochondrial activities.

Fig. S1. Characterization of β-cell subtypes derived from Myt1^{+}Ngn3^{+} (M^{+}N^{+}) and M^{-}N^{+} progenitors in *MNYA* mice. Related to Fig. 1. (a-c) Global distribution of lineage-labeled cells of M^{+}N^{+}-islet progenitor-derived islet (β) cells in MNYA (a, b) and *MNT* mice (c), using endogenous fluorescence (a, b) or IF (c). In a and b, Apple (red) marked β cells. eYFP (green) marked lineage-labeled β cells. In c, tdT (red) marked lineage-labeled cells. Insulin (green) labeled β cells. Islets of 6 mice were examined, yielding similar results. (d-h) Examination of the proportion of each islet cell type in pseudo-islets (PSI) made from sorted cells, with IF and quantification data shown. tdT (red) marked lineage-marked cells. Hormones (green or white) were labeled in each panel. In the quantification of e and h, mean +SEM were presented. Each dot represents one PSI. Islets were from 4 batches of sorted cells/PSIs. In e, 30 tdT+ and 46 tdT- PSIs were included. In h, 12 tdT+ and 17 tdT- PSIs were included. (j-n) Secretion of sorted β-cell subtypes using MNYA mice. (j) a typical FACS profile for β-cell subset collection, done 4 times with similar results. (k) Typical recovered PSIs, done 4 times with similar results. (l) GSIS from eYFP^{+} or eYFP^{-} pseudo-islets made from MNYI islet cells, including male and female cells. The % of total insulin secreted within a 45-minute window was presented, as (mean+ SEM). *P* value is from an unpaired t-test, two-sided type-two error. Each dot (total 6) represents one GSIS assay, from one batch of PSI of one sorted sample. (m, n) Control secretion assays using *Ins1^{Cre}* to activate tdT (m) or eYFP (n) in all islet β cells in *Ai9* and *R26R^{eYFP}* reporter mice. Mean + SEM are shown. *P*-values are from a t-test with a two-sided type-two error. Each dot represents one GSIS assay from one batch of islets (both males and females were put together). In m and n, 4 *Ins1^{Cre}, 4 Ai9; Ins1^{Cre}, and 8 R26R^{eYFP}; Ins1^{Cre}* samples were included.

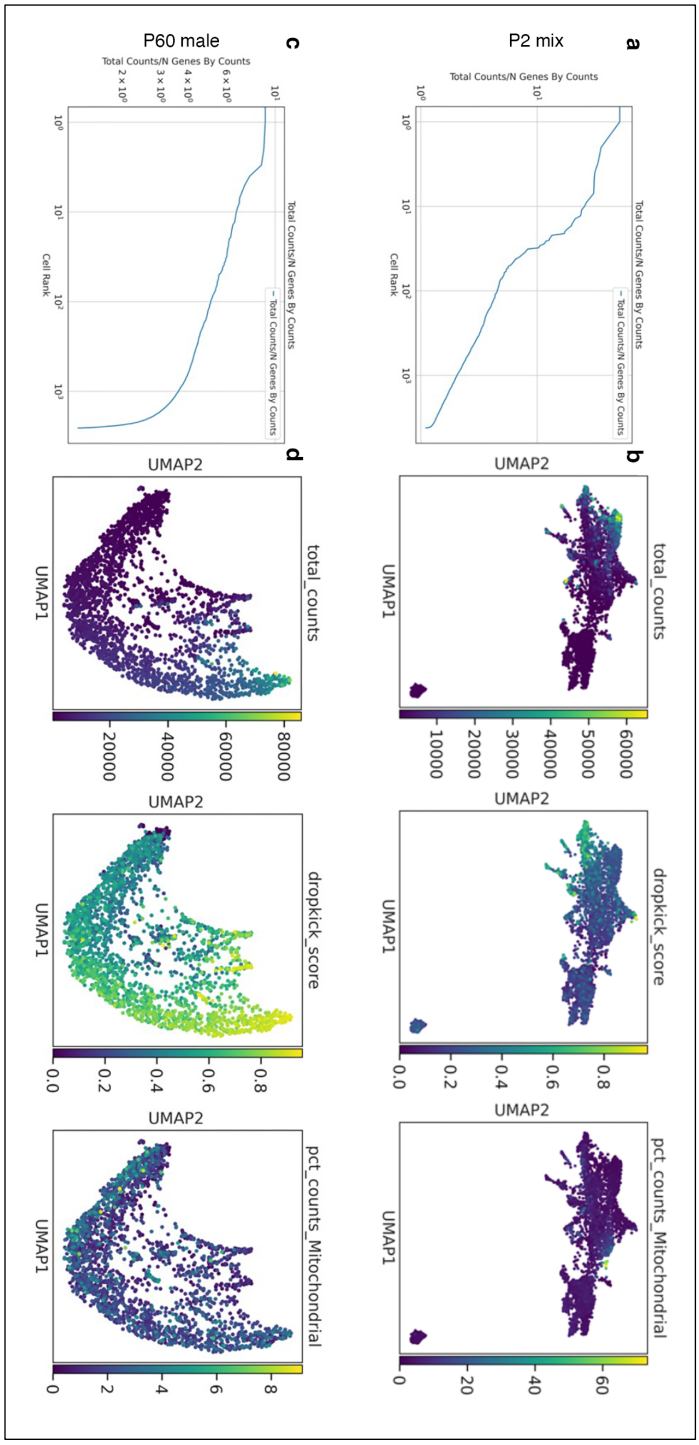

Fig. S2. Quality controls for sc-RNAseq in P2 and P60 β cells. Related to Fig. 2 and 3. (a) An example of cell ranking (based on the total number of counts/genes) in P2 islet cells. (b) More detailed quality controls using different criteria (from left to right: total counts per cell, a dropkick algorithm that removes poor quality cells, and normalized count over mitochondrial genes that eliminates dead cells). (c, d) An example of quality control for a P60 male islet sample. The layout follows that of P2.

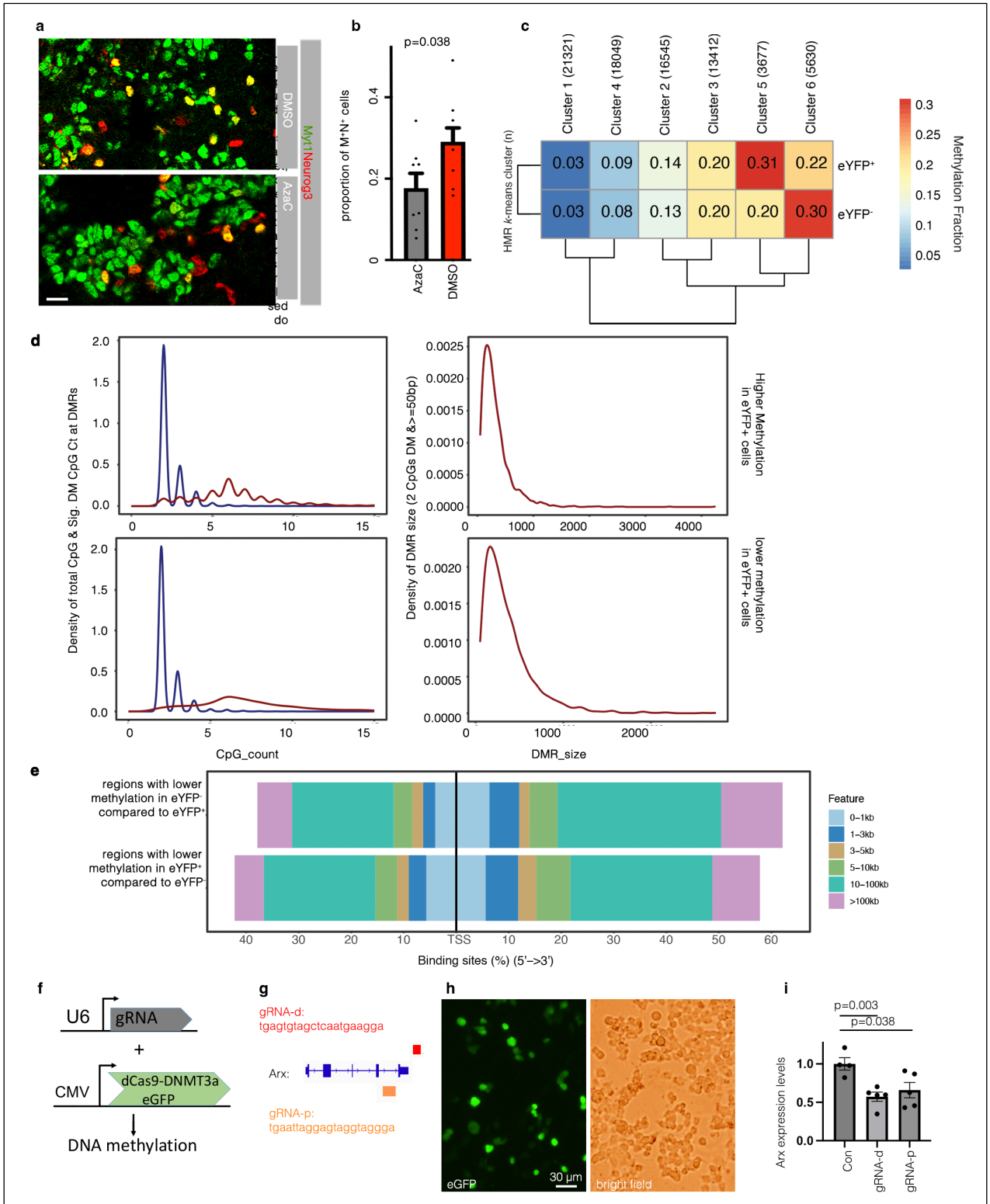

Fig. S3: DMRs between P2 β-cell subtypes.

Fig. S3. DMRs between P2 β-cell subtypes. Related to Fig. 4. (a, b) The effects of DNMT activity inhibition on the proportion of M^+N^+ progenitor cells in pancreatic bud culture. The quantification in b is mean + SEM, with p value from a t-test with a two-sided type-two error. Each dot represents one cultured bud. (c) *K*-means clustering (*k*=6) of all HMRs (n=78634) identified in P2 $eYFP^+$ and $eYFP^-$ β cell subtypes (from *MNYA* mice). The aggregated methylation fraction is displayed for all HMRs within each *k*-means cluster. (d) Properties of DMRs that have higher (top) or lower (bottom) methylation levels in M^+N^+ progenitor-derived β-cell subtypes ($eYFP^+$) relative to M^-N^+ progenitor-derived β-cell subtypes ($eYFP^-$). The left panels are density curves that represent the distribution of the total number of CpG dinucleotides (red line) and significantly (sig.) differentially methylated (DM) CpG counts (Ct, blue line) at identified DMRs. The right panels also have density curves that describe the size distribution of DMRs. (e) The proportion of DMRs mapping to specific distance windows relative to the TSS of their nearest gene. (f, e) A diagram showing the transcriptional constructs used to methylate the two DMRs near the *Arx* locus. The guide RNA (gRNA) sequences used were presented in g. Note that the two transcriptional units are contained in a single DNA plasmid. (h) An example of transfected αTC6 cells with a gRNA + CMV-dCAs9-DNMT3a-eGFP construct, shown by eGFP expression (green) 6 days after transfection. The individual eGFP fluorescence channel and a bright field channel are included. (i) RT-PCR assays (mean ± Sem) of *Arx* transcription after hypermethylation of DMRs, induced by the distal and proximal gRNA (6 days after transfection). The control is the empty construct without the gsRNA. P values are from a t-test with two-sided type-two errors. Each dot represents one independent transfection, with 4 controls and 5 methylation samples using each gRNA.

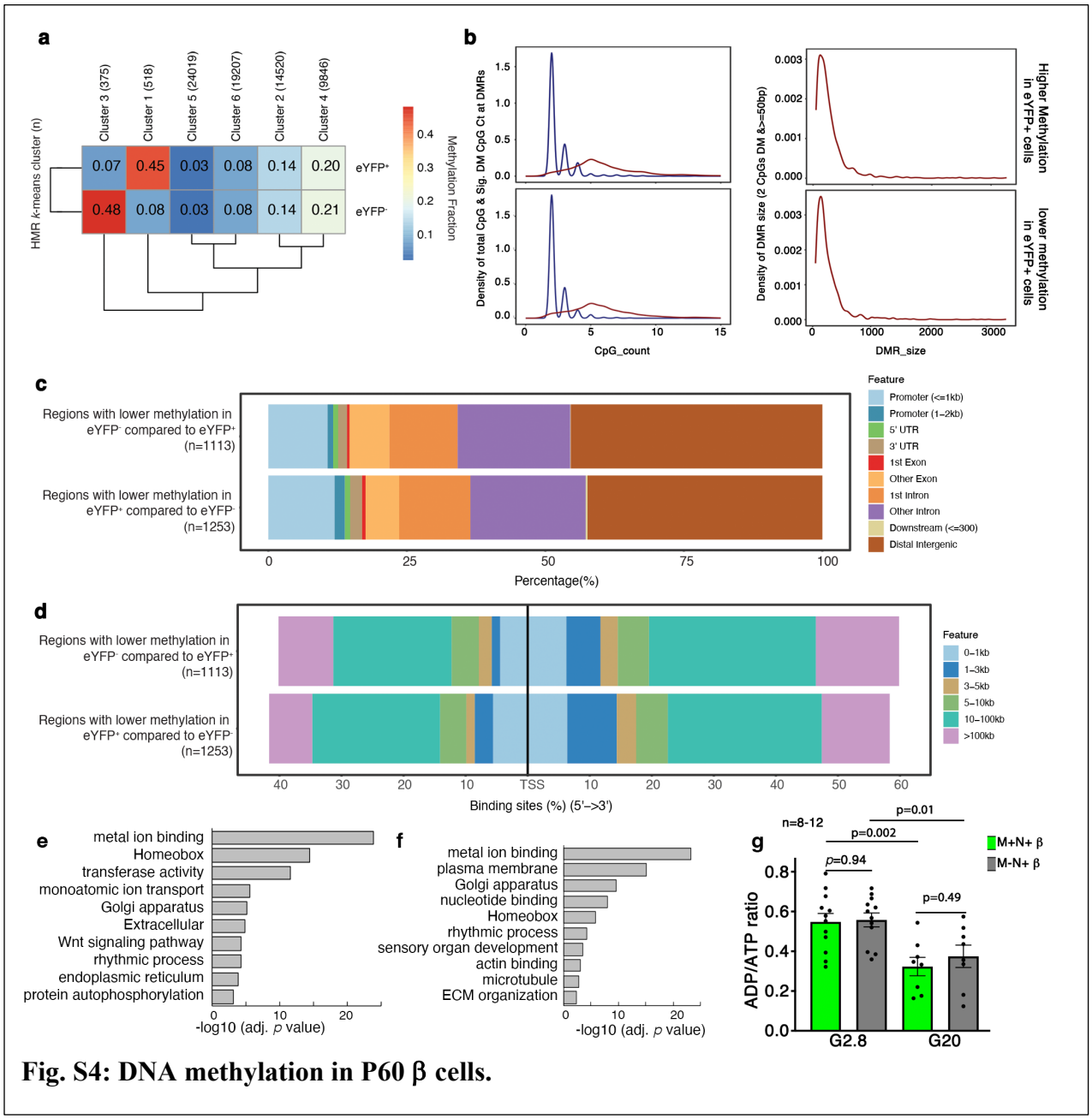

Fig. S4: DNA methylation in P60 β cells.

Fig. S4. Identification of DMRs between P60 β-cell subtypes. Related to Fig. 5. (a) *K*-means clustering (*k*=6) of all HMRs (n=68,485) identified in P6 eYFP$^+$ and eYFP$^-$ β cell subtypes (from *MNYA* mice). The aggregated methylation fraction is displayed for all HMRs within each *k*-means cluster. (b) Properties of DMRs that have higher (top) or lower (bottom) methylation levels in M$^+$N$^+$ progenitor-derived β cells (eYFP$^+$) relative to M$^-$N$^+$ progenitor-derived β-cells (eYFP$^-$). The left panels are density curves that represent the distribution of the total number of CpG dinucleotides (red line) and significantly (sig.) differentially methylated (DM) CpG counts (Ct, blue line) at identified DMRs. The right panels also have density curves that describe the size distribution of DMRs. (c) The proportion of DMRs overlapping different genomic annotations (promoter, intron, exon, intergenic regions, etc.). (d) The proportion of DMRs mapping to specific distance windows relative to the TSS of their nearest gene. (e, f) Gene Ontology (GO) terms identified via DAVID [21] using gene lists that are associated with DMRs that have higher (e) or lower (f) levels of DNA methylation in eYFP$^+$ β cell subtypes relative to eYFP$^-$ β cell subtypes (called using GREAT) [22]. P values were

from one-tailed analysis, adjusted using the Benjamini-Hochenberg procedure for multiple comparisons. (g) ADP/ATP ratios of two β-cell subtypes from two-month-old *MNYA* mice (mean + SEM) (both males and females). Each dot represents an assay from one individually sorted sample (12 samples for G2.8 and 8 samples for G20). P values are from a t-test with a two-sided type-two error.

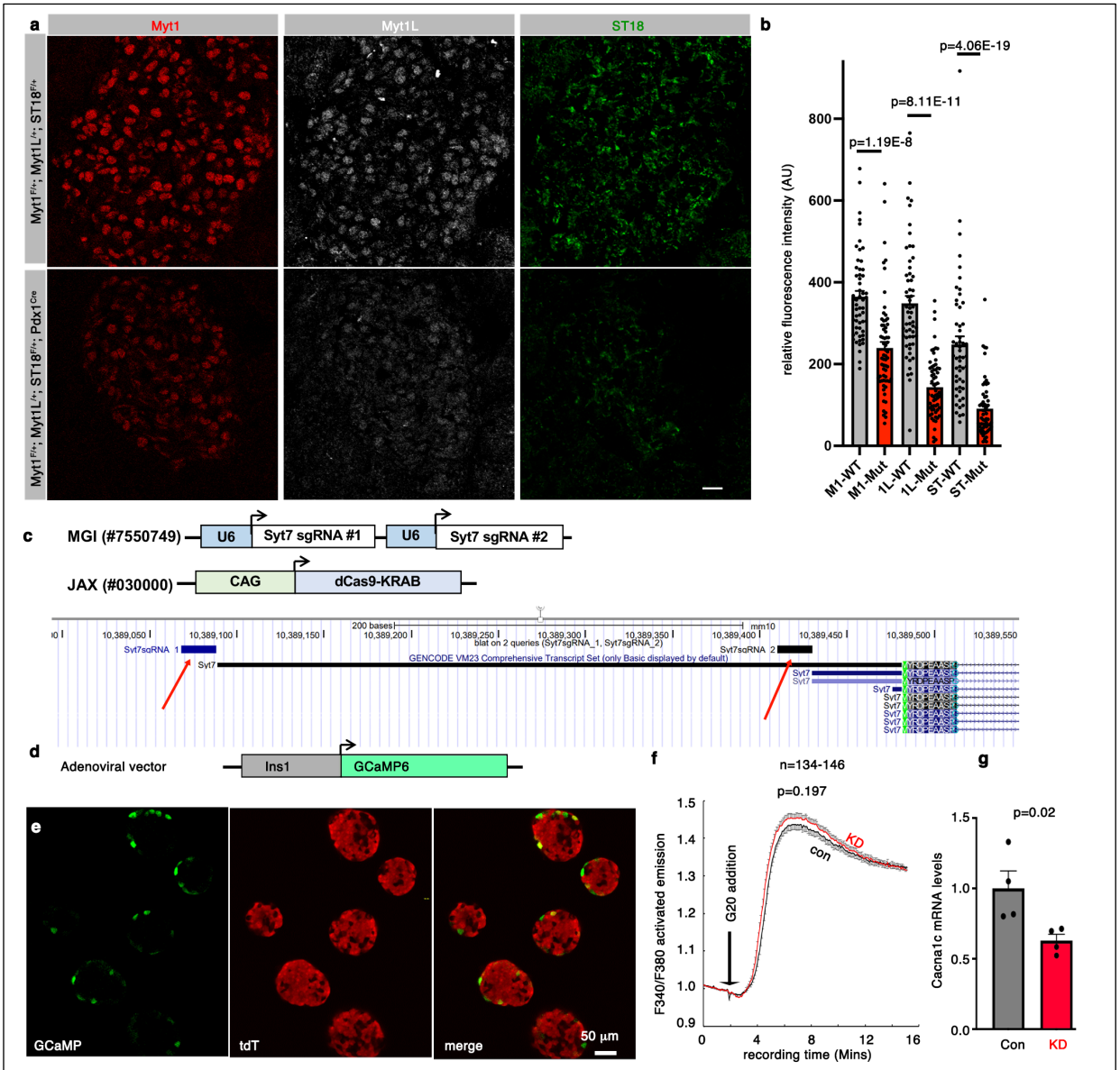

Fig. S5: Quality controls of human single β cells.

Fig. S5. Gene dosage manipulation followed by functional tests. Related to Fig. 6. (a, b) Immunofluorescence (IF) assays of Myt1 (M1), Myt1L (1L), and St18 (ST) levels (mean + SEM) in islets of P21 heterozygous mice. Shown in (b) are the average IF intensity per islet area (artificial units or A. U.). Each dot is one islet cell cluster, with 3 mice of each genotype used. P values are from t-tests with two-sided type-two errors. The total number of sections from left to right columns in b are: 56, 64, 57, 65, 54, and 58. (c) The transgene used for *Syt7* transcriptional repression based on CRISPRi (top). The locations of the two guide RNAs were marked (red arrows), in reference to the two transcriptional starting sites. (d) The construct used to express GCaMP6 specifically in β cells, using an adenoviral vector for delivery. (e) Still images of the MNT islet used for GCaMP6 recording, shown in Movie S1. The isolated islets were infected with an adenovirus that drives the expression of GCaMP6 with an Ins1 promoter/enhancer. (f, g) The effect of siRNA-based *Cacna1c* knockdown (KD) in primary islet β cells, assayed as pseudo-islets (PSI) (mean + SEM). (f) Aggregated Ca^{2+} influx in PSIs assayed with Fura2. P values are calculated using two-way ANOVA and repeated assays (with 134 controls and 146 KD PSIs of 4 batches of studies). (g) Real-time RT-PCR-based assay of the *Cacna1c* level reduction after transfection with control (con) and KD siRNAs 4 independent sets of samples were used. P values are from a t-test with two-sided type-two errors.

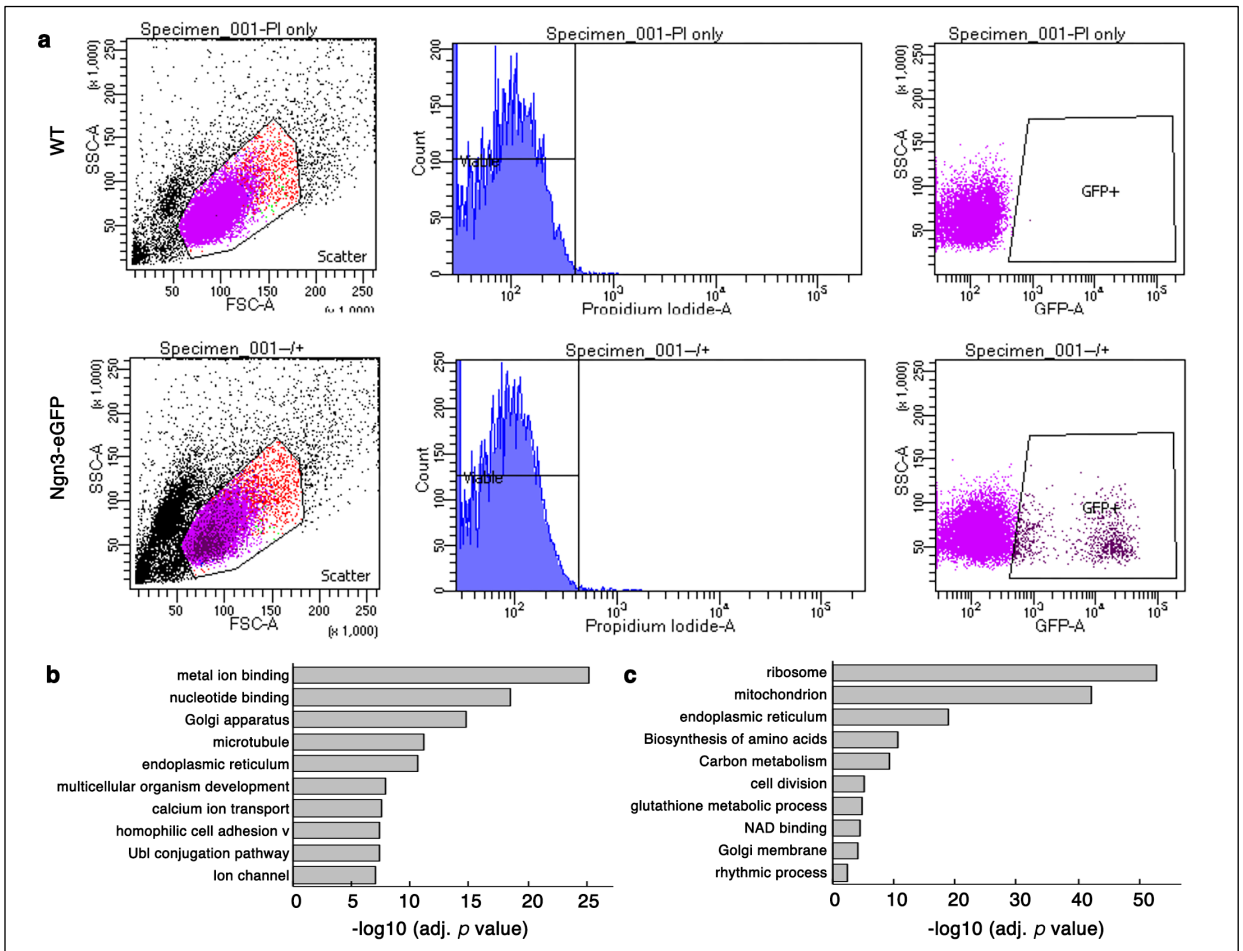

Fig. S6: The impact of mHFD on gene expression/genetic pathways of endocrine progenitors at E15.5.

Fig. S6. The impact of mHFD on endocrine progenitors' gene expression/genetic pathways at E15.5. Related to Fig. 7. (a) FACES controls for endocrine progenitor cell purification using *Ngn3*^{eGFP} mice. WT females (6-8 weeks old) were fed with HFD for 2 weeks. They were crossed with *Ngn3*$^{eGFP/+}$ males not exposed to HFD (while staying in HFD). E15.5 embryos were dissociated and sorted for RNAseq. (b, c) The terms associated with down- or up-regulated genes in mHFD-treated endocrine progenitors were analyzed via DAVID. P values were from t-test with one-tailed type-two errors, adjusted using the Benjamini-Hochenberg procedure for multiple comparisons.

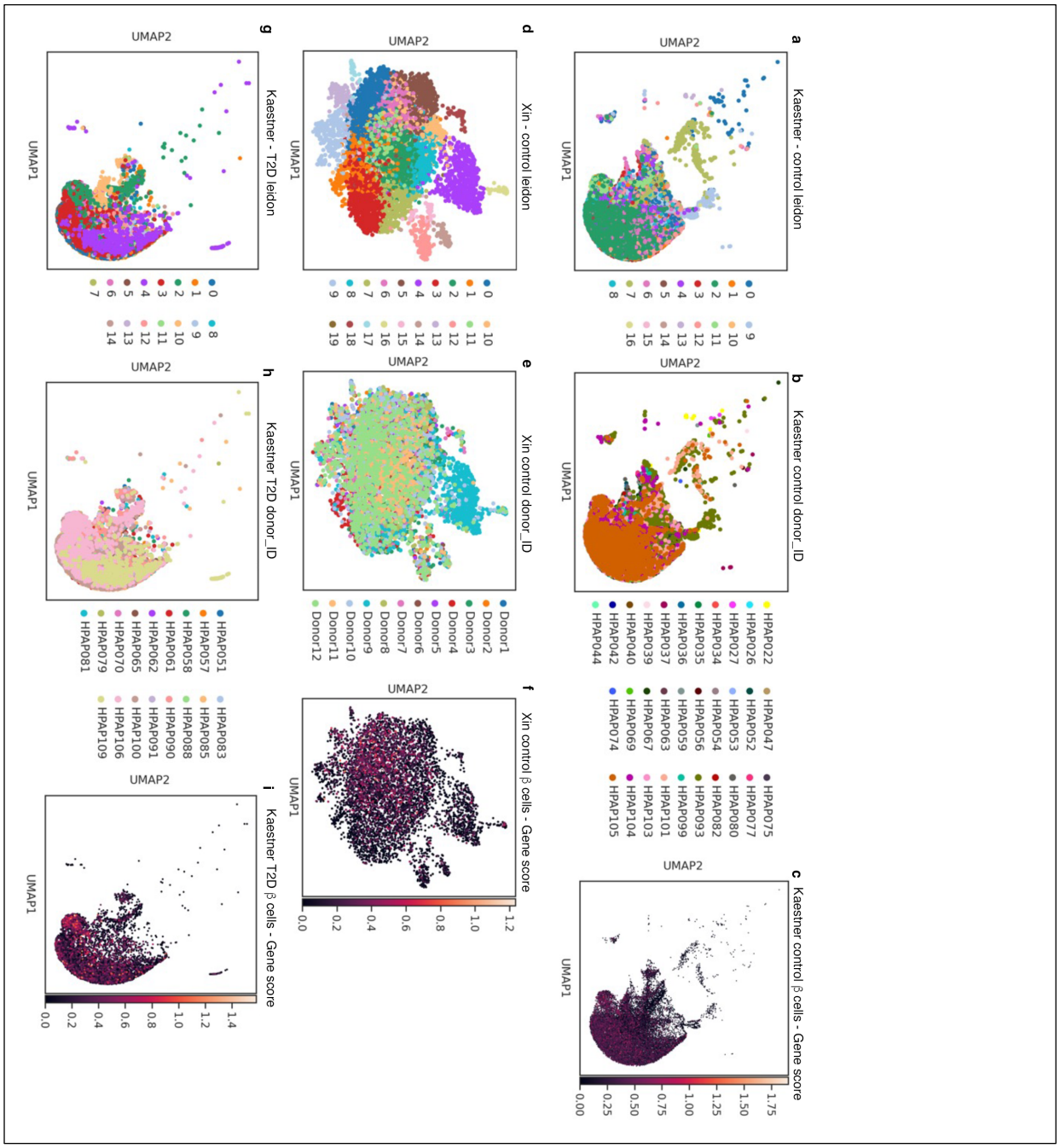

Fig. S7. Quality controls for sc-RNAseq data analysis of human donor islets. Related to Fig. 7. (a-c) Cell clustering using different algorithms (a, leidon). Overlapped cells from ID-ed donors (b, showing variabilities amongst donors), and gene score (c, used in figures). Panels (d-f) and (g-i) are similar to (a-c), except that different islet preps were used.

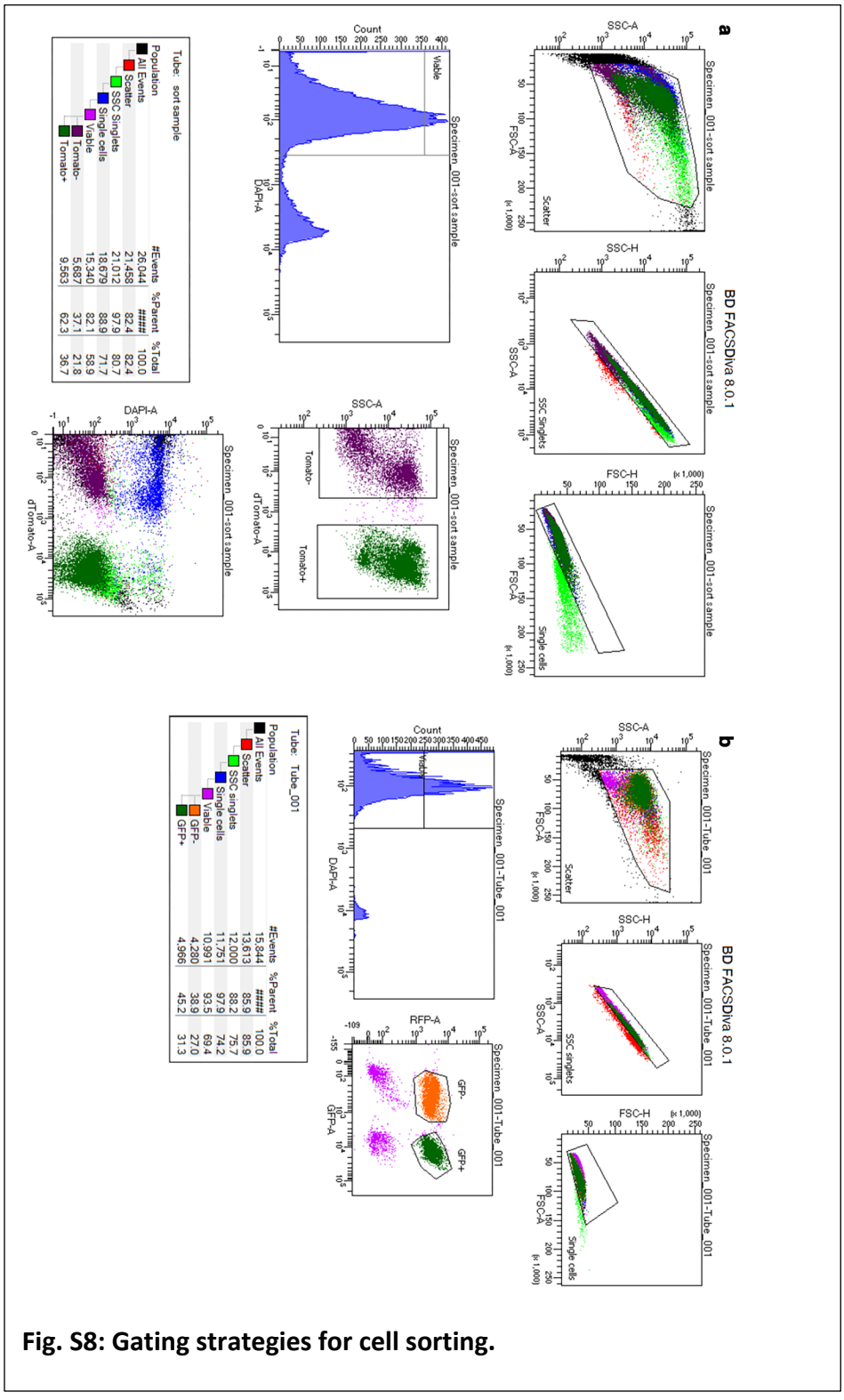

Fig. S8: Gating strategies for cell sorting.

Fig. S9. Gating strategies for cell sorting. (a) Gating for tdT+ and tdT- cell sorting using MNT islets. (b) Gating strategy for sorting eYFP^{+} and eYFP^{-} β cells using *MNYA* mice.

1. Liu, J. *et al.* Neurog3-Independent Methylation Is the Earliest Detectable Mark Distinguishing Pancreatic Progenitor Identity. *Dev Cell* **48**, 49-63 e47 (2019).
2. Wollam, J. *et al.* Chromogranin A regulates vesicle storage and mitochondrial dynamics to influence insulin secretion. *Cell Tissue Res* **368**, 487-501 (2017).
3. Vera, M. *et al.* The translation elongation factor eEF1A1 couples transcription to translation during heat shock response. *Elife* **3**, e03164 (2014).
4. Sehrawat, U. *et al.* Inhibitors of eIF4G1-eIF1 uncover its regulatory role of ER/UPR stress-response genes independent of eIF2alpha-phosphorylation. *Proceedings of the National Academy of Sciences of the United States of America* **119**, e2120339119 (2022).
5. Taneera, J. *et al.* GNAS gene is an important regulator of insulin secretory capacity in pancreatic beta-cells. *Gene* **715**, 144028 (2019).
6. Weiske, J. & Huber, O. The histidine triad protein Hint1 triggers apoptosis independent of its enzymatic activity. *J Biol Chem* **281**, 27356-27366 (2006).
7. Haase, M. & Fitze, G. HSP90AB1: Helping the good and the bad. *Gene* **575**, 171-186 (2016).
8. Kim, S.J. *et al.* Mitochondrial peptides modulate mitochondrial function during cellular senescence. *Aging (Albany NY)* **10**, 1239-1256 (2018).
9. Wang, X. & Jiang, L. Effects of ornithine decarboxylase antizyme 1 on the proliferation and differentiation of human oral cancer cells. *Int J Mol Med* **34**, 1606-1612 (2014).
10. Liu, T. *et al.* Pax6 directly down-regulates Pcsk1n expression thereby regulating PC1/3 dependent proinsulin processing. *PLoS One* **7**, e46934 (2012).
11. Jonsson, A. *et al.* Effect of a common variant of the PCSK2 gene on reduced insulin secretion. *Diabetologia* **55**, 3245-3251 (2012).
12. Rajkumar, K. *et al.* Understanding perspectives of signalling mechanisms regulating PEBP1 function. *Cell Biochem Funct* **34**, 394-403 (2016).
13. Khandelwal, P. *et al.* Rab11a-dependent exocytosis of discoidal/fusiform vesicles in bladder umbrella cells. *Proceedings of the National Academy of Sciences of the United States of America* **105**, 15773-15778 (2008).
14. Zabetian-Targhi, F., Mahmoudi, M.J., Rezaei, N. & Mahmoudi, M. Retinol binding protein 4 in relation to diet, inflammation, immunity, and cardiovascular diseases. *Adv Nutr* **6**, 748-762 (2015).
15. Wang, M., Parshin, A.V., Shcherbik, N. & Pestov, D.G. Reduced expression of the mouse ribosomal protein Rpl17 alters the diversity of mature ribosomes by enhancing production of shortened 5.8S rRNA. *RNA* **21**, 1240-1248 (2015).
16. Peisker, K. *et al.* Ribosome-associated complex binds to ribosomes in close proximity of Rpl31 at the exit of the polypeptide tunnel in yeast. *Mol Biol Cell* **19**, 5279-5288 (2008).
17. Xu, J., Su, X., Burley, S.K. & Zheng, X.F.S. Nuclear SOD1 in Growth Control, Oxidative Stress Response, Amyotrophic Lateral Sclerosis, and Cancer. *Antioxidants (Basel)* **11** (2022).
18. Wu, B. *et al.* Synaptotagmin-7 phosphorylation mediates GLP-1-dependent potentiation of insulin secretion from beta-cells. *Proc Natl Acad Sci U S A* **112**, 9996-10001 (2015).
19. Thomas, D.D., Frey, C.L., Messenger, S.W., August, B.K. & Groblewski, G.E. A role for tumor protein TPD52 phosphorylation in endo-membrane trafficking during cytokinesis. *Biochem Biophys Res Commun* **402**, 583-587 (2010).

20. Ma, Y. Tpt1 the balance toward immunosuppression upon cell death. *Nat Immunol* **22**, 940-942 (2021).
21. Sherman, B.T. *et al.* DAVID: a web server for functional enrichment analysis and functional annotation of gene lists (2021 update). *Nucleic Acids Res* **50**, W216-W221 (2022).
22. McLean, C.Y. *et al.* GREAT improves functional interpretation of cis-regulatory regions. *Nat Biotechnol* **28**, 495-501 (2010).